Recent Results on Hadronic B Decays from CLEO

Roy A. Briere
Harvard University
HEP Lab
42 Oxford St.
Cambridge, MA 02138

Several recent measurements of hadronic B decays from CLEO are discussed. These include modes of interest for CP violation studies, and others with implications for charm-counting.

1 Introduction

We review some recent measurements from CLEO. These include measurements of the branching ratios for $B \to \psi K^{(*)}$, the first full angular fit to the ψK^* decay, and upper limits for $B \to D^{(*)+}D^{(*)-}$. All of these modes are of interest for CP-violation studies. In addition, we present measurements of the inclusive rates for $B \to D^{(*)}X$. These are of great importance for 'charm-counting' in B decays. We briefly discuss charm-counting, including new opportunities using flavor-tagged rates.

2 CESR and CLEO

The Cornell Electron Storage Ring (CESR) is a symmetric e^+e^- collider operating at $\sqrt{s} \simeq 10.6$ GeV with world-record luminosity.

The CLEOII detector, described in detail elsewhere,[1] is a 4π collider detector with three concentric drift chambers in a 1.5T magnetic field. We use dE/dx and time-of-flight for particle identification. An excellent CsI electromagnetic calorimeter and a muon detection system complete the detector.

We take data in two modes. 'Continuum', or off-resonance, running results in:

$$e^+e^- \to \gamma^* \to e^+e^-, \mu^+\mu^-, \tau^+\tau^-, u\bar{u}, d\bar{d}, s\bar{s}, c\bar{c} \tag{1}$$

and also, $\gamma\gamma \to X$. 'On-resonance' running makes use of the $\Upsilon(4s)$ resonance to make $B\bar{B}$ pairs:

$$e^+e^- \to \gamma^* \to \Upsilon(4s) \to B\bar{B} \tag{2}$$

in addition to the normal continuum processes. The B mesons are quite soft, with $|P_B| \simeq 340$ MeV/c. The CLEOII dataset consists of $3.2 fb^{-1}$ on-resonance and $1.6 fb^{-1}$ continuum running, plus various special runs.

The currently operating CLEO2.5 upgrade has taken more than $2fb^{-1}$ of physics data so far, of an expected total of $> 5fb^{-1}$. The upgrade includes a new beam pipe and a silicon vertex detector, as well as a new drift-chamber gas (helium-propane). This data is not used in the results presented here.

3 Full Reconstruction of B Mesons

The technique of fully reconstructing B decays at the $\Upsilon(4s)$ is important for several of the analyses discussed. CESR's beam energies are well-known, and constrain B candidates to obey $E_B = E_{beam}$. Two key variables, expressing energy and momentum conservation, help to identify good B candidates.

First, consider:

$$\Delta E \equiv \sum E_i - E_{beam} \tag{3}$$

where i labels the decay products. This quantity peaks at zero for real events, and is sensitive to particle mis-identification and missing particles.

Second, we calculate the candidate 'beam-constrained' mass as:

$$M_B \equiv \sqrt{E_{beam}^2 - \left|\sum \vec{P}_i\right|^2} \tag{4}$$

Using E_{beam} in place of $\sum E_i$ here improves the mass resolution by about a factor of 10 in typical two-body decays.

4 $B \to \psi K^{(*)}$ Physics

$B \to \psi K_S$ is of interest to measure CP-violation, in particular the CKM unitarity triangle angle β. $B \to \psi K^*$ can *also* be used, *if* we can deal with the mixture of CP-odd and CP-even decays.

We perform a full angular fit to $B \to \psi K^*$ for the first time, using the complex amplitudes (four independent parameters after fixing one phase and the total rate):

$$A_0, A_\parallel \qquad \text{combinations of } S-\text{and } D-\text{wave}; \quad CP-\text{even}. \tag{5}$$

$$A_\perp \qquad P-\text{wave}; \quad CP-\text{odd} \tag{6}$$

The magnitude of $A_\perp$ allows us to measure the 'CP-purity' of the final state. Relative phases among the A_i would imply final-state interactions, and hence non-factorizable contributions.

Assuming factorization, one can predict $\Gamma_L/\Gamma = |A_0|^2$ and $R \equiv \mathcal{B}(B \to \psi K^*)/\mathcal{B}(B \to \psi K)$. Previous results have been somewhat inconsistent or imprecise.

5 $B \to \psi K^{(*)}$ Analysis

Our electron identification uses E/p and dE/dx, while our muon identification uses penetration into the muon system. For K (K^*) modes, we require one (both) lepton(s) to be identified. The K modes have low background, so the looser cuts are useful to increase our efficiency.

The ψ mass cuts are -150 MeV/c^2 $< m_{ee} - m_\psi <$ 45 MeV/c^2 and -45 MeV/c^2 $< m_{\mu\mu} - m_\psi <$ 45 MeV/c^2. A kinematic fit (which does not affect the angles) improves the E_ψ resolution by more than a factor of 5. All angular resolutions are ≤ 0.06 radian.

We use $K^{*+} \to K^+\pi^0, K_S\pi^+$ and $K^{*0} \to K^+\pi^-, K_S\pi^0$, requiring the K^* mass to be within 75 MeV/c^2 of the nominal value. Feed-across among K^* modes is suppressed with a decay angle cut; this suppresses soft π^0's, which have large background.

The B is fully reconstructed. We cut on $\Delta E \equiv |E_{cand} - E_{beam}| < 30 - 60$ MeV; this mode-dependent cut is chosen to be about 3 standard deviations. Our reconstruction efficiencies range from 9% to 48%.

The ψK^* decays require three angles to fully specify. We use the 'transversity angle' basis[2] for our angular fits, which also include the mass, M_B, to normalize the total rate.

6 $B \to \psi K^{(*)}$ Results

The B-mass distribution for the ψK modes are shown in Fig. 1; projections of the ψK^* angular fit are displayed in Fig. 2. Numerical results from the ψK^* angular fit are presented in Table 1 and branching fractions for all modes are summarized in Table 2.

The small value of $|P|^2$ is good news for CP-violation studies – the final state is almost a pure CP eigenstate. Also, since the A_i are real, within errors, we have no evidence yet for large final-state interactions.

Table 1: Results of the ψK^* angular fit.

Parameter	Value
$\lvert A_0\rvert^2 = \Gamma_L / \Gamma$	$0.52 \pm 0.07 \pm 0.04$
$\lvert A_\perp\rvert^2 = \lvert P\rvert^2$	$0.16 \pm 0.08 \pm 0.04$
$\phi(A_\perp)$	$-0.11 \pm 0.46 \pm 0.03$ radian
$\phi(A_\parallel)$	$3.00 \pm 0.37 \pm 0.04$ radian

The K^* mass distribution is displayed in Fig. 3. There is an excess of data above the $K^*(892)$, showing up in all modes, but we cannot yet distinguish

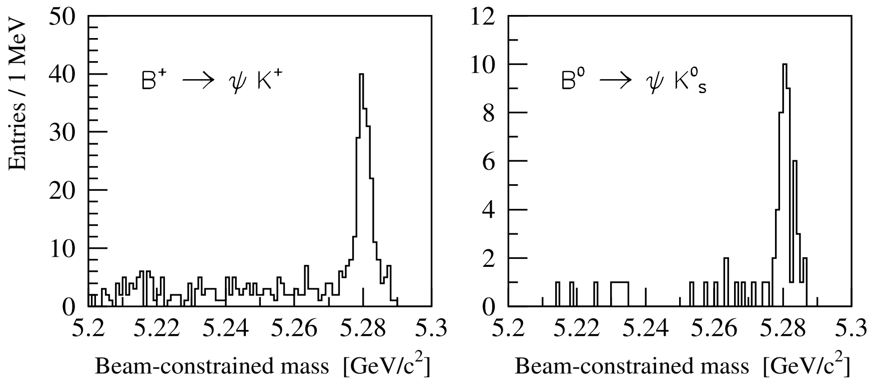

Figure 1: Beam-constrained mass distributions for $B^+ \to \psi K^+$ and $B^0 \to \psi K^0_S$.

Table 2: Measured signal yields and branching fractions.

Decay mode	Signal Yield	Branching Fraction $[10^{-3}]$
$B^+ \to \psi K^+$	198.1 ± 14.9	$1.02 \pm 0.08 \pm 0.07$
$B^0 \to \psi K^0$	$45.5\ ^{+7.3}_{-6.6}$	$0.85\ ^{+0.14}_{-0.12} \pm 0.06$
$B^+ \to \psi K^{*+}$	42.5 ± 7.1	$1.41 \pm 0.23 \pm 0.24$
$B^0 \to \psi K^{*0}$	81.6 ± 10.3	$1.32 \pm 0.17 \pm 0.17$

resonances from non-resonant $K\pi$. A conservative systematic error is used to allow for events under the K^* peak from this excess.

The dominant systematic errors for the K modes are tracking and particle ID efficiency, and knowledge of $\mathcal{B}(\psi \to \ell\ell)$. For the K^* modes, feed-across between modes and non-resonant $K\pi$ dominate.

We also extract:

$$R \;=\; \mathcal{B}(B \to \psi K^*)/\mathcal{B}(B \to \psi K) \;=\; 1.45 \pm 0.20 \pm 0.17 \tag{7}$$

Γ_L/Γ (see Table 1) and R are now in better agreement with expectations from naive factorization.

Assuming $\Gamma(B^+ \to \psi K^{(*)+}) = \Gamma(B^0 \to \psi K^{(*)0})$, we obtain:

$$(f_{+-}\tau_{B^+})/(f_{00}\tau_{B^0}) \;=\; 1.15 \pm 0.17 \pm 0.06. \tag{8}$$

This measurement currently provides our best knowledge of the production fraction ratio for B mesons at the $\Upsilon(4s)$, f_{+-}/f_{00}, since the ratio τ_{B^+}/τ_{B^0}, which is consistent with unity, is more precisely known.[3]

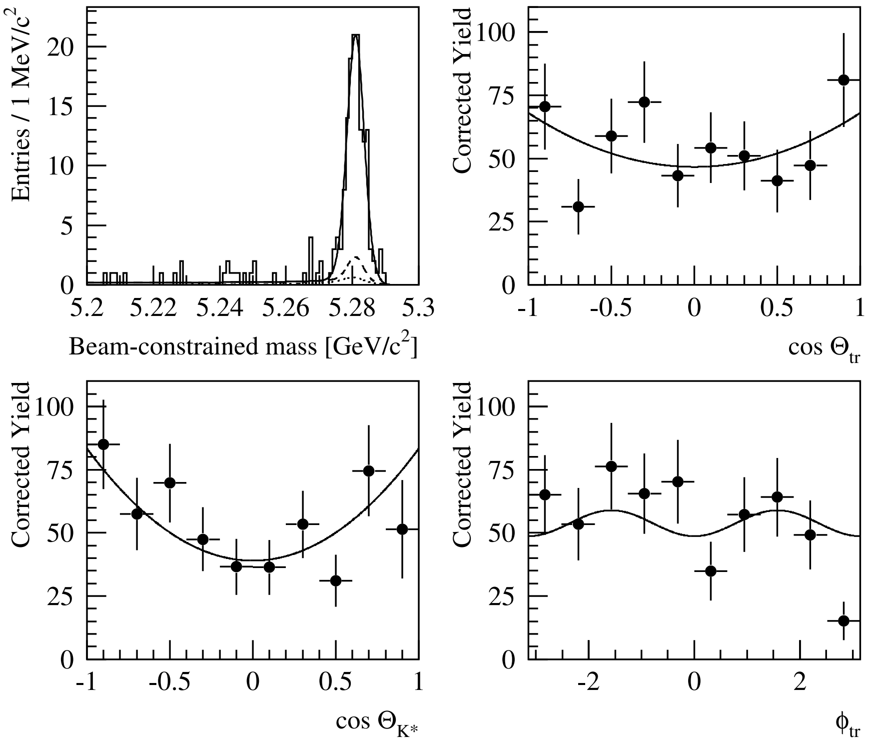

Figure 2: One-dimensional projections of the full 4-D fit. The mass plot shows the data (histogram), the fit (solid line), the sum of all backgrounds (dashed) and the feed-across (dotted). The angular plots are acceptance-corrected.

7 $B \to D^{(*)+}D^{(*)-}$ Analysis

The decay $B \to D^{(*)+}D^{(*)-}$ also has sensitivity to the unitarity triangle angle β. We expect branching ratios of $\mathcal{O}(10^{-3})$.

The analysis includes event shape for continuum suppression and basic track quality cuts. Particle identification is from dE/dx and time-of-flight.

We use the decay modes: $D^{*+} \to D^0\pi^+$, $D^+ \to K^-\pi^+\pi^+$, and $D^0 \to K^-\pi^+, K^-\pi^+\pi^0, K^-\pi^-\pi^+\pi^+$. A Dalitz-plot cut for $K^-\pi^+\pi^0$ enhances the signal-to-noise for this sub-mode. The $M_{D^*} - M_D$ resolution is improved with a kinematic fit. A decay angle cut for the π from D^* in D^*D mode helps suppress background. Finally, we cut on a total summed χ^2 from D masses and $D^* - D$ mass differences.

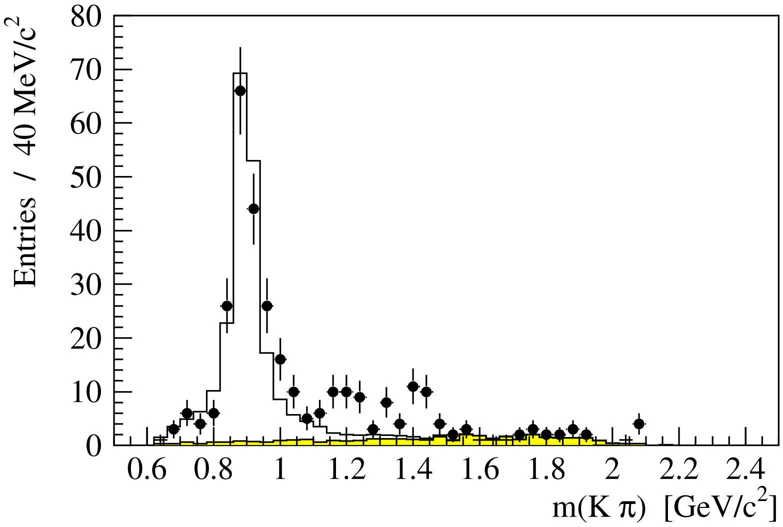

Figure 3: The $K\pi$ mass distribution for $m_B > 5.27$ GeV/c^2. Empty histogram: $K^*(892)$ mass from fit (incl. feed-across) Shaded histogram: combinatorial background

The cuts are tuned to give the lowest probability of background fluctuating to expected signal for a 0.1% branching ratio. Cuts of two standard deviations are placed on ΔE and M_B. The background is estimated from ΔE sidebands.

8 $B \to D^{(*)+}D^{(*)-}$ Results

In $D^{*+}D^{*-}$, we observe one event with an expected background of 0.022 ± 0.011 events; see Fig. 4. We quote an upper limit here; however, the event is 'golden'.

The other modes are consistent with expectations from background. We arrive at the following upper limits:

- $\mathcal{B}(B^0 \to D^{*+}D^{*-}) < 2.2 \times 10^{-3}$ 90% CL
- $\mathcal{B}(B^0 \to D^{*+}D^{*+} + D^+D^{*-}) < 1.8 \times 10^{-3}$ 90% CL
- $\mathcal{B}(B^0 \to D^+D^-) < 1.2 \times 10^{-3}$ 90% CL

9 $B \to D^{(*)}X$ Analysis

Measurements of $\mathcal{B}(B \to D^{(*)}X)$ are an important input for charm-counting – an accounting of how b quarks decay. Note that we do not correlate the flavor

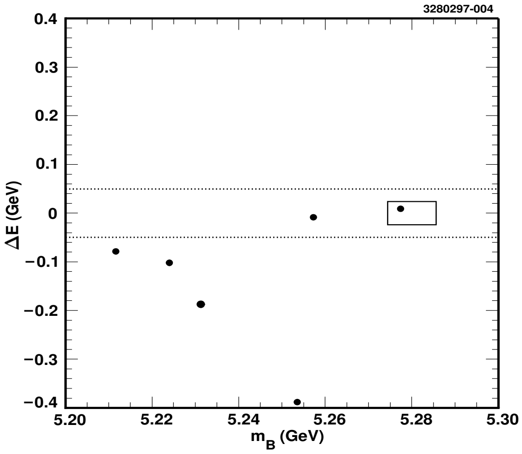

Figure 4: B-mass - ΔE distribution for $B^0 \to D^{*+}D^{*-}$.

of the B and D in this analysis; we will discuss such separation below.

The analysis cuts are simple. We use event-shape cuts suppress continuum. Track quality cuts are imposed, and loose dE/dx is used for particle ID. All γ's are required to be in a good fiducial region, with $E_\gamma > 30MeV$. We use the decay modes: $D^0 \to K^-\pi^+$; $D^+ \to K^-\pi^+\pi^+$; $D^{*+} \to D^0\pi^+$; $D^{*0} \to D^0\pi^+, D^+\pi^0$. We employ CLEO branching ratios for these modes to allow a cleaner treatment of common systematic errors.

The D^* modes are quite clean. The D^+ channel has background from $D_s^+ \to K^+K^-\pi^+$; this small effect is included in the fits via Monte-Carlo.

For the D^0 analysis, we take care in treating $K-\pi$ swapping, which yields a false and broader mass peak, and K^+K^-, $\pi^+\pi^-$, $K^-\pi^+\pi^0$ which contribute satellite peaks in mass. These momentum-dependent effects are illustrated in Figs. 5 and 6. The D^0 result was cross-checked by an analysis with tighter particle ID cuts, which removed the bulk of these complications. The results are in excellent agreement.

10 $B \to D^{(*)}X$ Results

Mass peaks are fit for each momentum bin (20 bins for D^0, 10 bins for the others); we then sum the acceptance-corrected yields. Much work is done to assure unbiased fits. The total number of B decays is determined from luminosity and our measured $\Upsilon(4s)$ cross-section.

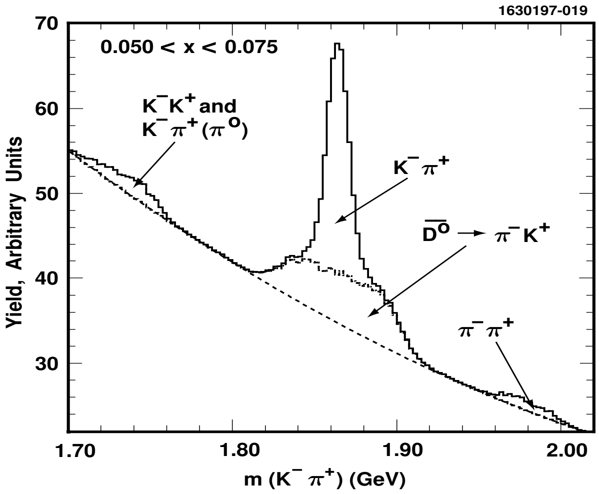

Figure 5: Low-momentum $K\pi$ mass showing components. Here, $x \equiv P_{K\pi}/P_{max}$, where $P_{max} = \sqrt{E_{beam}^2 - M_D^2}$.

We obtain the branching ratios:

- $\mathcal{B}(B \to D^0 X) = 0.636 \pm 0.014 \pm 0.019 \pm 0.018$
- $\mathcal{B}(B \to D^+ X) = 0.235 \pm 0.009 \pm 0.009 \pm 0.024$
- $\mathcal{B}(B \to D^{*0} X) = 0.247 \pm 0.012 \pm 0.018 \pm 0.018$
- $\mathcal{B}(B \to D^{*+} X) = 0.239 \pm 0.011 \pm 0.014 \pm 0.009$

The errors are statistical, systematic, and $D^{(*)}$ branching ratios, respectively.

Our D^{*0}/D^{*+} ratio is consistent with isospin: $\mathcal{B}(B \to D^{*0}X)/\mathcal{B}(B \to D^{*+}X) = 1.03 \pm 0.07 \pm 0.09 \pm 0.08$. We also measured the momentum spectrum for each $D^{(*)}$ species, and the D^* polarizations as a function of momentum.

11 Conventional Charm Counting

It is interesting to sum inclusive modes with charm and calculate n_c, the number of $c + \bar{c}$ quarks per b decay. There has been a shortfall in n_c for some time. Given $\mathcal{B}(B \to X\ell\nu)$, which is affected by the total hadronic width, one expects $n_c \simeq 1.3$. One cannot easily explain both n_c and $\mathcal{B}(B \to X\ell\nu)$. There is now interest in $b \to c\bar{c}s$ hadronization as a possible clue to a resolution.[4]

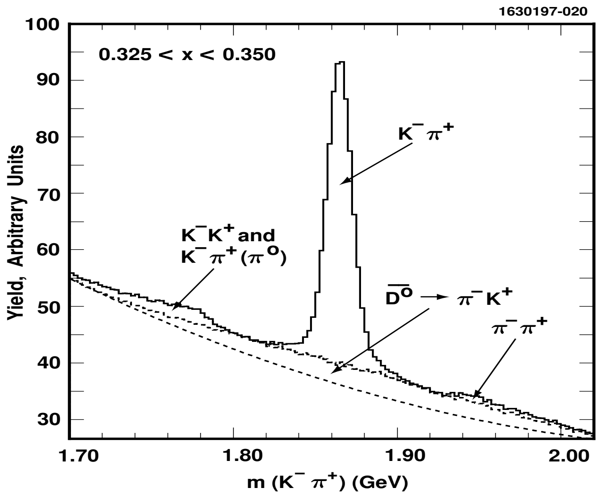

Figure 6: High-momentum $K\pi$ mass showing components. Here, $x \equiv P_{K\pi}/P_{max}$, where $P_{max} = \sqrt{E_{beam}^2 - M_D^2}$.

Our $\mathcal{B}(B \to D^{(*)}X)$ results are a great improvement over the current PDG values. The resulting updated reckoning is presented in Table 3: we find that the shortfall persists.

Table 3: Input Values for Charm Counting.

Mode	Rate	Comments
$D^{0,+}X$	0.871 ± 0.035	New CLEO
$D_s X$	0.118 ± 0.031	CLEOII D_sX + $\mathcal{B}(D_s \to \phi\pi)$
$\Lambda_c X$	0.039 ± 0.020	unpublished
$\Xi_c^+ X$	0.008 ± 0.005	corrected
$\Xi_c^0 X$	0.012 ± 0.009	corrected
$2 \times c\bar{c}X$	0.054 ± 0.007	η_c upper limit
SUM	1.102 ± 0.052	

Unfortunately, such counting is not without its share of subtle issues. We therefore review the particular choices that have been made. In addition to our $D^{(*)}X$ results, we use CLEO's latest $\mathcal{B}(B \to D_sX)$ and our new, model-independent $\mathcal{B}(D_s \to \phi\pi) = (3.6 \pm 0.9)\%$. We use an unpublished CLEO thesis result for $\Lambda_c X$ and the world average $\mathcal{B}(\Lambda_c \to pK\pi)$. The Ξ_cX values are corrected for $\Gamma(\Xi_c \to X\ell\nu)/\Gamma(D \to X\ell\nu) \simeq 2.5 \pm 1.0$,[5] which was originally taken as 1. We also take $\Gamma(\Xi_c \to \Xi\ell\nu)/\Gamma(\Xi_c \to X\ell\nu) \simeq 0.8 \pm 0.2$. Finally, we use the upper limit for $\eta_c X$ in place of the sum of all unmeasured charmonium modes.

12 Flavor-Tagging and Charm Counting

In addition to the non-flavor-specific $B \to D^0 X$ result presented above, flavor-specific results are also recently available. These permit fresh new views of charm counting. Using D-ℓ correlations, CLEO has measured:[6]

$$\mathcal{B}(\bar{B} \to \bar{D}X)/\mathcal{B}(\bar{B} \to DX) = (10.7 \pm 0.29 \pm 0.18)\% \qquad (9)$$

The lepton tags one B, while the angular correlation tells if D and ℓ are from same B. With this and other measurements, one can now look at flavor-tagged charm yields for the first time. There are now also related measurements available from ALEPH and DELPHI.

Recently, one group has made novel use of the flavor-tagged inclusive charm rates.[7] They calculate $\mathcal{B}(b \to \text{no open charm})$ in two ways: first, by counting c in $b \to c$ (Method A), and second, by counting $\bar{c}$ in $b \to c\bar{c}s$ (Method B). These should be consistent. Note that 'open charm' denotes a particle with charm quantum number $C = \pm 1$.

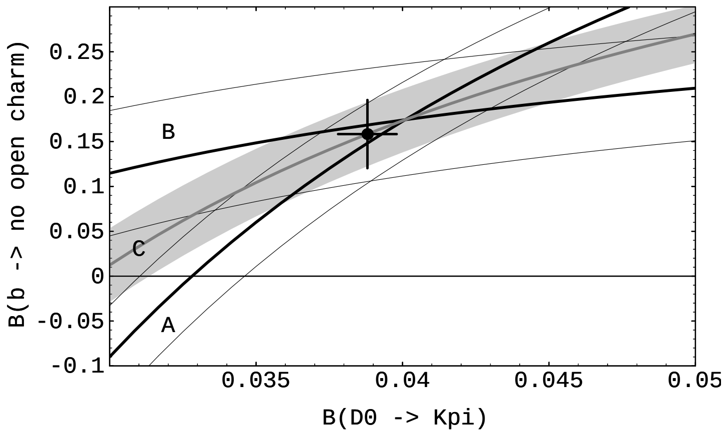

Figure 7: Flavor-specific counting. (courtesy Dunietz, et al.)

This particular study shows that the two methods are self-consistent with a conventional value of $\mathcal{B}(D^0 \to K^-\pi^+)$. But, it implies a much larger that expected $\mathcal{B}(b \to \text{no open charm})$.

Different input assumptions may yield other conclusions; the real point is that data now exist to do such studies!

13 Related Pursuits for the Near Future

Many other related analyses are underway at CLEO. These include:

- New CLEO2.5 data for $\psi K^{(*)}$ and $D^{(*)+}D^{(*)-}$ studies.
- A check of $\mathcal{B}(D^0 \to K^-\pi^+)$.
- Updates of flavor-tagged charm yields.
- A measurement of $\mathcal{B}(B \to D_{s1}X)$.
- Exclusive reconstruction of $\bar{B} \to D^{(*)}\bar{D}^{(*)}\bar{K}^{(*)}$.
- Updates of $D^{(*)}\pi^{(*)}$ modes.

14 Conclusions

New CLEO results on hadronic B decays were presented. We examined both $\psi K^{(*)}$ and $D^{(*)+}D^{(*)-}$, which are of interest for CP-violation studies. Our results for $\mathcal{B}(B \to D^{(*)}X)$ allow an update of charm counting, which is still interesting and puzzling, but new flavor-tagged information can give new insights. Much current interest is focused on the $b \to c\bar{c}s$ transition. We expect further CLEO contributions to all of these topics.

References

1. Y. Kubota, *et al.*, *Nucl. Instrum. Methods* A**320**, 66 (1992).
2. A.S. Dighe, I. Dunietz, H.J. Lipkin and J.L. Rosner, Phys. Lett. **B369**, 144 (1996).
3. Review of Particle Physics, R.M Barnett, *et al.*, Phys. Rev. D **51** 1 (1996).
4. Gerhard Buchalla, Isard Dunietz and Hitoshi Yamamoto, Phys. Lett. **B364** 188 (1995).
5. M.B. Voloshin, Phys. Lett. **B385**, 369 (1996); and M.B. Voloshin, private communication.
6. CLEO Collaboration, Rencontres de Moriond 1996, Les Arcs, France; presented by Y. Kwon.
7. I. Dunietz, et al., hep-ph/961242.